NASA TECHNICAL NOTE

NASA TN D-2762

NASA TN D-2762

MAXIMUM LIFT-DRAG RATIOS OF DELTA-WING—HALF-CONE COMBINATIONS AT A MACH NUMBER OF 20 IN HELIUM

by Patrick J. Johnston, Curtis D. Snyder, and Robert D. Witcofski

Langley Research Center
Langley Station, Hampton, Va.

NATIONAL AERONAUTICS AND SPACE ADMINISTRATION • WASHINGTON, D. C. • MAY 1965

NASA TN D-2762

MAXIMUM LIFT-DRAG RATIOS OF DELTA-WING–HALF-CONE COMBINATIONS AT A MACH NUMBER OF 20 IN HELIUM

By Patrick J. Johnston, Curtis D. Snyder,
and Robert D. Witcofski

Langley Research Center
Langley Station, Hampton, Va.

NATIONAL AERONAUTICS AND SPACE ADMINISTRATION

For sale by the Clearinghouse for Federal Scientific and Technical Information
Springfield, Virginia 22151 – Price $1.00

MAXIMUM LIFT-DRAG RATIOS OF DELTA-WING—HALF-CONE COMBINATIONS AT A MACH NUMBER OF 20 IN HELIUM

By Patrick J. Johnston, Curtis D. Snyder,
and Robert D. Witcofski
Langley Research Center

SUMMARY

Maximum lift-drag ratios of a family of delta-wing—half-cone combinations have been determined experimentally at a Mach number of 20 in helium. Reynolds numbers based on overall length varied from 2.75×10^6 to 4.35×10^6. The semiapex angles of the delta wing ranged from 9° to 25° and the apex angles of the half-cone body ranged from 3° to 9°. Performance measurements were made with the bodies situated both above and beneath the wing.

The results showed that for a given wing-fuselage combination the performance of the flat-bottom configuration was always superior to that of the same configuration inverted. Increasing the half-cone angle invariably resulted in a deterioration in performance of flat-top configurations of fixed wing geometry. For flat-bottom configurations an increase in half-cone angle was accompanied by a reduction in maximum lift-drag ratios for the more slender wings; however, little or no reduction in performance occurred for the wings with 20° and 25° semiapex angles. For a given cone the most significant gains in performance occurred when the wing semiapex angle just exceeded the half-cone angle. The performance data of this investigation could be correlated on the basis of parameters suggested by linearized supersonic theory despite the fact that the Mach number was far beyond that for which linear theory is expected to apply.

INTRODUCTION

In contrast to the extensive research effort devoted to determining the performance of a multitude of configurations having relatively low hypersonic lift-drag ratios, the efforts devoted in recent years to the systematic investigation of those shapes capable of high lift-drag ratios have been meager. Much of what is presently known about the state of the art concerning configurations developing high lift-drag ratios at Mach numbers up to 10 is summarized in references 1 and 2. A more recent examination of problems concerning the aerodynamics of hypersonic cruise and boost vehicles is given in reference 3. Additional information on the effects of certain geometrical variations on maximum lift-drag ratios may be gleaned from an experimental investigation conducted at a Mach number of 8 and reported in reference 4. With but

few exceptions, all the data obtained in references 1 to 4 were limited to Mach numbers less than 10 inasmuch as wind-tunnel facilities capable of generating flow at higher Mach numbers were not available until recently.

The experimental data obtained in the investigations previously noted suggest that the advantages of utilizing favorable lift interference to increase maximum lift-drag ratios of winged vehicles might disappear at Mach numbers on the order of 10 and that beyond this Mach number, the flat-top orientation (body situated beneath the wing) and the flat-bottom orientation (body above the wing) will result in essentially equal maximum lift-drag ratios. Performance estimations such as those employed in reference 1 predict the proper magnitude of the maximum lift-drag ratio but do not predict the effects of body orientation on the maximum lift-drag ratio. Further, when these performance estimates were carried out at Mach numbers up to 17 the results indicated equivalent maximum lift-drag ratios for both flat-top and flat-bottom configurations. Thus, uncertainty still exists as to whether the favorable lift interference effects suggested in reference 5 will occur well into the hypersonic Mach number regime or whether this interference scheme tends to diminish as Mach number increases.

With these uncertainties in mind, therefore, the present investigation was undertaken to determine the performance of a family of delta-wing—half-cone combinations in order to ascertain whether favorable lift interference exists at Mach numbers in the neighborhood of 20. The investigation was conducted in the Langley 22-inch helium tunnel. The semiapex angles of the wing varied from 9° to 25°, and the apex angles of the right-circular half-cone body varied from 3° to 9°. The angles of attack ranged from -15° to 15° so as to encompass the angle at which the maximum lift-drag ratio occurs for configurations with the body situated both above and beneath the wing. Results were also obtained on the half-cone bodies alone. The Reynolds numbers based on the overall length ranged from 2.75×10^6 to 4.35×10^6.

SYMBOLS

b	span, in.
C_D	drag coefficient, $\frac{\text{Drag}}{qS}$
$C_{D,o}$	drag coefficient at $\alpha = 0^\circ$
C_L	lift coefficient, $\frac{\text{Lift}}{qS}$
$C_{L,opt}$	optimum lift coefficient, C_L at $(L/D)_{max}$
C_{L_α}	lift-curve slope, $\frac{dC_L}{d\alpha}$, per deg

c_r	root chord, in.
L/D	lift-drag ratio
$(L/D)_{max}$	maximum lift-drag ratio
M	Mach number
p_t	stagnation pressure, psig
q	dynamic pressure, psia
R	Reynolds number based on overall length
S	planform area, sq in.
t	wing thickness, in.
t_{le}	wing leading-edge thickness, in.
V	total volume of configuration, cu in.
α	angle of attack, deg
α_{opt}	optimum angle of attack, α at $(L/D)_{max}$, deg
ϵ	semiapex angle of wing, deg
θ	apex angle of half-cone body, deg

CONFIGURATIONS

A sketch of a representative model of the present investigation is shown in figure 1 along with a table listing the important physical dimensions of the wings. As indicated in the sketch, the models consisted of right-circular half-cone bodies attached to the flat side of delta wings. The apex angles of the half-cone body were 3°, 4°, 5°, 7.5°, and 9°, and the semiapex angles of the wing were 9°, 15°, 20°, and 25°. The wing surface opposite the body was fabricated with a 1° bevel in planes parallel to the plane of symmetry. The wing leading edges were square.

The small variations in the ratios of wing thickness to root chord and of leading-edge thickness to root chord shown in the table of figure 1 resulted from the fact that the models of the present investigation were scaled up from similar models designed for a smaller wind tunnel in which the wing thickness and leading-edge thickness were arbitrarily chosen to be 1/16 inch and 0.010 inch, respectively, for all wings. Further, the scale factors for a given wing could not be held fixed for the present models. (Note, for example,

that the wings having a 9° semiapex angle had root chords varying from 12.30 to 21.00 inches.) This variation in length was brought about by a compromise among several factors, the most important of which are as follows: (1) For the wings with larger semiapex angles, the span (and, hence, the root chord) was limited to insure that the wing tips would not protrude into the tunnel-wall boundary layer. (2) In those cases where the apex angle of the half-cone body was small (3° and 4°), the overall length was determined by the diameter of the cavity in the model required for the strain-gage balance and its location inside the half-cone body. (3) The remaining compromise as to model size was based upon considerations of the maximum load capacity of the strain-gage balance and tunnel stagnation pressures at which a calibration of the flow in the test section was available.

APPARATUS AND TESTS

The investigation was carried out in the Langley 22-inch helium tunnel. A contoured, axisymmetric nozzle was employed in the tests. This nozzle was designed to generate a uniform flow at a Mach number of 22; calibrations of the test-section flow, however, have indicated a dependence of nominal stream Mach number on stagnation pressure as indicated in the following table:

p_t, psig	M
500	19.1
750	19.9
1000	20.4

Other details concerning the operating capability of this facility may be found in reference 6; calibrations of the flow in the test region are available in reference 7.

The angles of attack of the models were referenced to the flat surface of the wings for the wing-body combinations and to the flat surface of the half-cone bodies for the isolated-body tests. The pitch attitude of the models was measured by an optical system and automatically recorded. The system consisted of a small lens-prism assembly mounted in the body, a point source of light positioned outside the test-section window, and a plate to which photoelectric cells were attached at calibrated intervals. As the light beam reflected by the prism passed each photocell, an electrical relay was energized and caused a high-speed analog to digital data recording system to sample and record the strain-gage-balance outputs on magnetic tape. During the course of each test, the outputs of the strain-gage balance were sampled twice at each photocell: once when the model was being pitched in the positive sense and again when the model was being pitched negatively. Although this technique allowed the model to be pitched continuously (thus, shortening the test duration and subsequent pump-up time between tests), its accuracy in angle of attack is limited and varied from test to test depending on the arrangement of the optical system. These uncertainties made it difficult to determine α_{opt} with any degree of

precision; however, $(L/D)_{max}$ could be determined satisfactorily from drag polars. Experience with this data-acquisition system has shown that when drag polars are employed, the scatter in $(L/D)_{max}$ due to uncertainties caused by the photocells is substantially reduced.

All tests were conducted at the nominal stagnation pressures listed in the previous table. Stagnation temperatures were near ambient at the beginning of each test but decreased about 20° F during the test as a result of the falling reservoir pressure. The Reynolds numbers based on model length corresponding to the aforementioned temperatures and pressures are listed in table I.

Separate tests were made to measure the base pressure for the purpose of adjusting the axial-force data to a condition where free-stream pressure acts over the base of the half-cone bodies. For these pressure measurements a differential-pressure transducer was employed. Thin-wall, 0.090-outside-diameter tubing was taped to the model support sting and extended from the model base region to the sensing side of the transducer located outside the strut section of the tunnel. A pressure of less than 10 microns of mercury was maintained on the reference side of the transducer. The model was held at a fixed angle of attack for each test until the pressure sensed by the transducer reached equilibrium. For these measurements the output of the transducer was recorded on oscillograph paper and the pressure usually stabilized after about 10 to 12 seconds. Care was taken to outgas the tubing on the sensing side of the transducer between tests.

RESULTS AND DISCUSSION

Effect of Body Size on Maximum Lift-Drag Ratio

The maximum lift-drag ratios obtained at Mach numbers on the order of 20 for the four wings investigated are presented in figure 2, as a function of the apex angle of the half-cone body.

In order to provide an end point on the ordinate and to aid in fairing representative curves through the data, the maximum lift-drag ratios of flat-plate delta wings were computed by employing two-dimensional shock-expansion theory over the wings and assuming the existence of laminar boundary layers with adiabatic wall conditions. Boundary-layer displacement effects on the skin friction were accounted for by the method outlined in appendix C of reference 8. The pressure drag due to values of t_{le}/c_r of 0.0010, 0.0013, 0.0015, and 0.0018 (see table in fig. 1) for the wing semiapex angles of 9°, 15°, 20°, and 25°, respectively, was also included. According to the extrapolations of figure 2, the calculations appeared to give reasonable predictions of the maximum lift-drag ratios for the isolated wings; however, these calculated values represent idealized upper limits since, particularly in relation to the experimental data for the flat-bottom configuration, the effect of the 1° streamwise wedge angle of the wing was neglected. It may also be of interest to note that

these calculations predicted a maximum lift-drag ratio of about 5.9 for zero-thickness delta wings for the conditions shown in figure 2, that is, a Mach number of 20 and a Reynolds number, based on the overall length, of 3.5×10^6.

As indicated in table I and explained in a previous section, the experimental results were obtained at several values of Reynolds number. For presentation in figure 2, these data have been adjusted to a common Reynolds number of 3.5×10^6 by a method to be discussed in a following section.

The data shown in figure 2 indicate that at Mach numbers on the order of 20, favorable lift interference does not exist on the flat-top configurations and the flat-bottom configuration provides a higher $(L/D)_{max}$ than its inverted counterpart. In addition, increasing the apex angle of the half-cone body always resulted in a deterioration in the performance of both the flat-top and flat-bottom configurations. When the fuselage was situated above the wing, the effect of body size on maximum lift-drag ratio diminished with increasing wing semiapex angle such that $(L/D)_{max}$ of the $\epsilon = 25^\circ$ wing was only slightly affected, at least within the range of half-cone angles investigated. The relatively large deterioration in performance of the flat-bottom configurations with body size for the more slender wings in contrast to the small or negligible reduction for the 20° and 25° wings is interpreted as an indication of the degree of body shielding afforded by the wings.

The experimental data obtained on configurations incorporating a 5° half-cone body and wings having semiapex angles of 20° and 25° indicated that the body orientation had no apparent effect on $(L/D)_{max}$. This anomaly is believed due, however, to the extremely small axial forces acting on these particular models and reflects the accuracy to which these forces could be measured.

Effect of Wing Semiapex Angle on $(L/D)_{max}$

The effect of increasing the wing semiapex angle on $(L/D)_{max}$ of configurations having a fixed half-cone body is shown in figure 3. Unlike the data given in figure 2, the data of figure 3 have not been adjusted to one Reynolds number; this does not obscure the fact that the significant gains in performance over $(L/D)_{max}$ for the isolated body are achieved when the semiapex angle of the wing just exceeds the apex angle of the half-cone body. Continued increases in wing semiapex angles yield little or no improvement in $(L/D)_{max}$. (See, for example, the data for $\theta = 7.5^\circ$ and $\theta = 9^\circ$.) The data presented in this figure for the isolated bodies are consistent with the data obtained on the wing-body combinations; that is, the performance of the flat-bottom configuration is superior to that of the same configuration inverted.

Performance as a Function of the Volume Coefficient

The nondimensional volume coefficient $V^{2/3}/S$ has been employed in figure 4 in order to compare the results of the present investigation. This ratio is frequently employed as an independent parameter for comparing the performance

of hypersonic vehicles since, for such configurations, the payload of specified volume is generally contained in the configuration having the least surface area. Larger values of this parameter, therefore, indicate structurally compact configurations. As in figure 2, the calculated maximum lift-drag ratios of the isolated flat-plate wings (assumed, in the case of fig. 4, to have $V^{2/3}/S = 0$) have been employed as a guide in fairing the curves of figure 4. As might be anticipated, the trends of $(L/D)_{max}$ with volume coefficient shown in figure 4 are consistent with those previously demonstrated in figure 2 since, for a given wing, $V^{2/3}/S$ is directly proportional to the apex angle of the half-cone body. In interpreting the lift-drag-ratio data of figure 4, it should be recognized that the wings of higher semiapex angle were unduly penalized because of the powerful effect leading-edge drag had on $(L/D)_{max}$. The deleterious effect leading-edge drag had on performance is illustrated by the vertical displacement of the theoretically derived maximum lift-drag ratios of flat-plate wings.

The angle of attack at which maximum lift-drag ratio occurs is shown in figure 4(a) for the flat-top orientation, and although some scatter exists, the general trend, as represented by a fairing through the data obtained on a 9° wing, is toward smaller angles of attack for larger volume coefficients. This trend might be anticipated since the half-cone becomes the dominate geometric feature of these high-volume shapes and since according to impact theory the maximum lift-drag ratio of half-cones occurs near zero angle of attack.

The shielding effect of the wing on the body, discussed previously in connection with the L/D data of figure 2 for the flat-bottom configuration, is reflected again in the α_{opt} data of figure 4(b). For a given wing, larger angles of attack are required to achieve $(L/D)_{max}$ for configurations with higher volume coefficients. Of course, this trend results from the fact that, for a given wing, an increase in the volume coefficient reflects a larger body size and, consequently, greater angles of attack are required to shield the body from the flow.

Although the data presented in figure 4 show that the configurations with the slenderest wing provided the highest $(L/D)_{max}$ over the range of volume coefficients, they also exhibit the lowest value of optimum lift coefficient - a parameter especially important in the design of cruise vehicles. An examination of the optimum lift coefficients for vehicles with fixed maximum lift-drag ratios (fig. 5) shows that to achieve these lift-drag ratios the configurations with higher volume coefficients are handicapped by a reduction in optimum lift coefficient. The data of figure 4 show that considerable latitude is available in choosing a geometry capable of the fixed maximum lift-drag ratios of figure 5; however, inasmuch as large values of the ratio $V^{2/3}/S$ can be interpreted as being structually more efficient, it is likely, in view of the results presented in figure 5, that the trade-off between structural and aerodynamic efficiency can assume an important role in the final choice of cruise-vehicle geometry.

Performance of Half-Cone Bodies

The maximum lift-drag ratios of the half-cone bodies are shown as a function of the volume coefficient in figure 6. Whereas the performance continues to increase with reductions in $V^{2/3}/S$ for the wing-body combinations (as typified by the curves for the 9° delta wing), the performance of the half-cone bodies reaches a peak and then begins to diminish with continued reduction in $V^{2/3}/S$ or half-cone angle. This reduction in maximum lift-drag ratio is probably associated with the reduced lifting effectiveness of the more slender bodies. (The lift-curve slope of the 3° half-cone body, for example, was only 1/5 of its Newtonian value of 0.0031.) It is probable that since this loss in lift-curve slope is associated with the fact that the slender bodies are surrounded by relatively thick boundary layers, the lift-curve slopes as well as maximum lift-drag ratios of bodies with higher fineness ratios would be strongly dependent on Reynolds number.

Figure 6 shows that the performance of several of the half-cone bodies compares favorably with that of the winged configurations having equivalent volume coefficients. Thus, for volume coefficients on the order of 0.3, the half-cone may be an attractive shape since it is not encumbered with wings that are relatively ineffectual from the storage volume standpoint. Further, the winged vehicles would require greater thermal protection for leading edges. Of course, for vehicles intended to perform well throughout the speed range from hypersonic to landing speeds, the half-cone bodies would need some auxiliary devices such as extensible or variable-sweep wings to provide adequate performance and handling at low speeds.

Performance Correlation Based on Linear Theory

For a number of years it has been recognized that supersonic linear theory fails to predict the forces on a body at Mach numbers much in excess of 3. Despite this inadequacy, reference 3 shows that it is possible to employ a linear theory expression for maximum lift-drag ratio as the parameter for correlating the performance of a variety of configurations at Mach numbers as high as 10. The performance data obtained in the present investigation were correlated as a function of parameters suggested by linearized supersonic theory. Although more rigorous expressions suggested by various authors were examined, the most satisfactory correlation of the data is shown in figure 7 where the drag coefficient at zero angle of attack was employed in the correlating parameter.

The method of correlating maximum lift-drag ratios shown in figure 7 is a powerful one which facilitates the adjustment and comparison of experimental data obtained at different Reynolds numbers. As noted previously, such adjustments were employed herein to account for the variation in test Reynolds numbers. For these adjustments it was assumed that the lift-curve slope is invariant with Reynolds number and that $C_{D,o}$ could be extrapolated parallel to the

curve of the coefficient of laminar skin friction as a function of Reynolds number.

Theoretical Performance Prediction

In order to determine whether the maximum lift-drag ratios of flat-top and flat-bottom delta-wing—half-cone combinations could be successfully predicted at the high Mach numbers investigated, the performance of a representative configuration of this investigation was estimated by a method in which the half-cone body is assumed to remain at zero incidence in the local flow field of the wing. A complete description of this local-flow method may be found in appendix B of reference 1. For these performance estimates laminar boundary layer and adiabatic wall conditions were assumed to prevail over the entire model.

The results of these calculations are shown in figure 8 for the configuration incorporating a 15° semiapex wing and a 5° half-cone body. For the flat-top orientation the drag was accurately predicted whereas the lift was overestimated, the error becoming greater as angle of attack increases. The result of these predictions was, of course, an overestimation in the performance for the flat-top orientation.

When the body is situated on the leeward surface of the wing, both lift and drag are slightly underestimated such that the resulting lift-drag ratio is accurately (but fortuitously) predicted. Equal maximum lift-drag ratios were predicted for both flat-top and flat-bottom orientations; a similar deficiency in this method of estimating maximum lift-drag ratios was observed in reference 1 at Mach numbers of 6.8 and 9.6.

To date, it is not known for certain under what conditions of Mach number, angle of attack, and model geometry the double-shock flow patterns underneath flat-top configurations, assumed in the previous simplified analysis, will exist. One investigation of the pressure distribution about delta-wing—half-cone configurations at Mach numbers of 5 and 8 (ref. 9) showed the existence of the double-shock type of flow. The configurations, however, had relatively low fineness ratios. (The half-cone angle was 12.5° and the wing semiapex angles were 25° and 40°.) Other pressure measurements at Mach numbers from 3 to 6 (ref. 10) and at Mach numbers of 7 and 10 (ref. 11) indicate only the single-shock type of flow. Recent pressure measurements (as yet unpublished) obtained in the Langley 22-inch helium tunnel at $M = 20$ on a configuration having a 20° semiapex wing and a 7.5° half-cone body also indicate the existence of the single-shock type of flow. Similar results have also been reported in reference 4 at a Mach number of 21. Reference 4 also indicates that the introduction of a half-cone body underneath a delta wing causes a significant disturbance in the flow field all the way out to the wing leading edge instead of being confined to a rather limited region adjacent to the wing-body juncture. The results of these pressure measurements indicate that the nature of the flow beneath flat-top wing-body combinations is far more complex than assumed in the local-flow method of analysis, and it is reasonable, therefore, that this method of estimating performance gives poor results. It would appear that before precise performance estimates can be made on flat-top orientations,

detailed pressure measurements will be necessary in order to establish the conditions under which the variety of flow patterns, such as those suggested in reference 12, will exist beneath flat-top configurations.

CONCLUDING REMARKS

Measurements of the maximum lift-drag ratios are presented for a family of delta-wing—half-cone combinations at a Mach number in the neighborhood of 20. The results indicate that, without exception, the flat-bottom orientation provided higher maximum lift-drag ratios than the corresponding flat-top configuration. The addition of body volume in the form of increasing the half-cone angle always resulted in a deterioration of performance for the flat-top configurations. Within the range of model geometries of this investigation, an increase of body volume was not always accompanied by a reduction in the performance of the flat-bottom configuration. For example, those configurations with slender wings exhibited a substantial loss in performance with increases in body volume whereas little or no reduction in maximum lift-drag ratio could be detected for configurations having wing semiapex angles of 20° and 25°.

For a fixed body size, the results indicated that the significant gains in performance for both flat-top and flat-bottom orientations occurred when the wing semiapex angle only slightly exceeded the half-cone angle; further increases in wing semiapex angle yielded little or no improvement in performance. The performance of several of the half-cone bodies compares favorably with that of the winged configurations for certain values of the ratio of volume to planform area. The maximum lift-drag ratio could be correlated on the basis of parameters suggested by linearized supersonic theory even though the data were obtained at a Mach number far beyond that for which linear theory could be expected to apply.

Langley Research Center,
National Aeronautics and Space Administration,
Langley Station, Hampton, Va., January 28, 1965.

REFERENCES

1. Armstrong, William O.; and Ladson, Charles L. (With Appendix A by Donald L. Baradell and Thomas A. Blackstock): Effects of Variation in Body Orientation and Wing and Body Geometry on Lift-Drag Characteristics of a Series of Wing-Body Combinations at Mach Numbers From 3 to 18. NASA TM X-73, 1959.

2. McLellan, Charles H.; and Ladson, Charles L.: A Summary of the Aerodynamic Performance of Hypersonic Gliders. NASA TM X-237, 1960.

3. Bertram, Mitchel H.; Fetterman, David E., Jr.; and Henry, John R.: The Aerodynamics of Hypersonic Cruising and Boost Vehicles. Proceedings of the NASA-University Conference on the Science and Technology of Space Exploration, Vol. 2, NASA SP-11, 1962, pp. 215-234. (Also available as NASA SP-23.)

4. Mead, Harold R.; Koch, Frank; and Hartofilis, Stavros A.: Theoretical Prediction of Pressures in Hypersonic Flow With Special Reference to Configurations Having Attached Leading-Edge Shock - Part III. Experimental Measurements of Forces at Mach 8 and Pressures at Mach 21. ASD TR 61-60, Pt. III, U.S. Air Force, Oct. 1962.

5. Eggers, A. J., Jr.; and Syvertson, Clarence A.: Aircraft Configurations Developing High Lift-Drag Ratios at High Supersonic Speeds. NACA RM A55L05, 1956.

6. Johnston, Patrick J.; and Snyder, Curtis D.: Static Longitudinal Stability and Performance of Several Ballistic Spacecraft Configurations in Helium at a Mach Number of 24.5. NASA TN D-1379, 1962.

7. Arrington, James P.; Joiner, Roy C., Jr., and Henderson, Arthur, Jr.: Longitudinal Characteristics of Several Configurations at Hypersonic Mach Numbers in Conical and Contoured Nozzles. NASA TN D-2489, 1964.

8. Bertram, Mitchel H.: Boundary-Layer Displacement Effects in Air at Mach Numbers of 6.8 and 9.6. NASA TR R-22, 1959. (Supersedes NACA TN 4133.)

9. Mead, Harold R.; and Koch, Frank: Theoretical Prediction of Pressures in Hypersonic Flow With Special Reference to Configurations Having Attached Leading-Edge Shock - Part II. Experimental Pressure Measurements at Mach 5 and 8. ASD TR 61-60, Pt. II, U.S. Air Force, May 1962.

10. Savin, Raymond C.: Approximate Solutions for the Flow About Flat-Top Wing-Body Configurations at High Supersonic Airspeeds. NACA RM A58F02, 1958.

11. Dunavant, James C.: Heat Transfer to a Delta-Wing—Half-Cone Combination at Mach Numbers of 7 and 10. NASA TN D-2199, 1964.

12. Scheuing, Richard A.; Brook, John W.; et al.: Theoretical Prediction of Pressures in Hypersonic Flow With Special Reference to Configurations Having Attached Leading-Edge Shock - Part I. Theoretical Investigation. ASD TR 61-60, Pt. I, U.S. Air Force, May 1962.

TABLE I.- MODEL CONFIGURATIONS AND TEST CONDITIONS

ϵ, deg	θ, deg	M	c_r, in.	R	$\frac{V^{2/3}}{S}$
9	3	19.1	21.00	4.35×10^6	0.1106
	4	19.1	15.75	3.06	.1486
	5	19.9	12.30	3.58	.1907
	7.5	19.9	12.30	3.48	.3000
	9	19.9	12.30	3.49	.3733
15	4	19.2	15.75	3.18×10^6	0.0999
	5	19.9	12.30	3.56	.1207
	7.5	19.9	12.30	3.46	.1839
	9	19.9	12.30	3.45	.2265
20	5	20.3	8.00	2.91×10^6	0.1001
	7.5	20.4	8.00	2.94	.1445
	9	20.4	8.00	2.92	.1751
25	5	20.3	8.00	2.91×10^6	0.0857
	7.5	20.3	8.00	2.75	.1192
	9	20.4	8.00	2.89	.1424
Isolated half-cones	3	19.1	21.00	4.22×10^6	0.2431
	4	19.1	15.75	3.21	.2677
	5	19.9	12.30	3.40	.2885
	7.5	19.8	12.30	3.42	.3308
	9	19.8	12.30	3.41	.3515

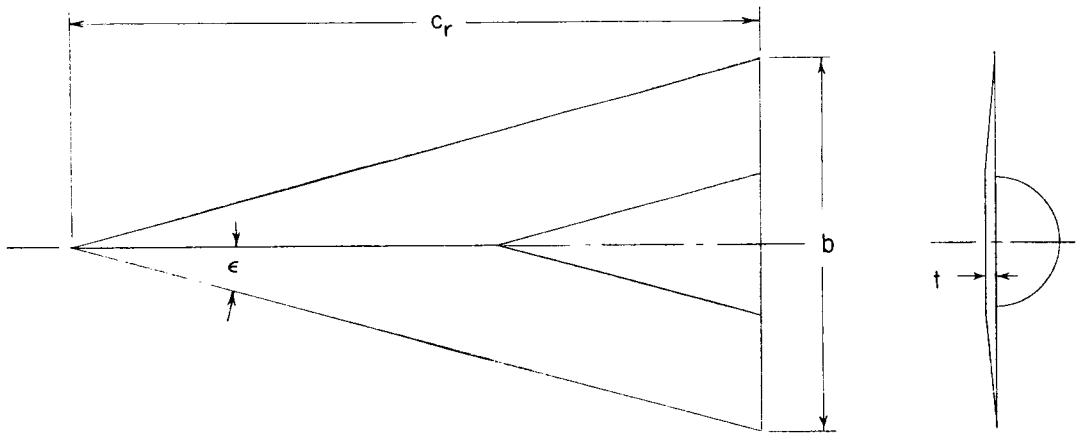

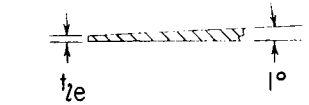

Wing leading-edge detail parallel to plane of symmetry

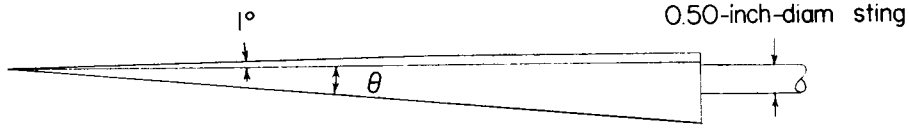

ϵ	c_r, in.	b, in.	t/c_r	t_{le}/c_r
9°	21.00	6.652	.0075	.0010
	15.75	4.989	.0098	.0013
	12.30	3.896	.0128	.0017
15°	15.75	8.440	.0098	.0013
	12.30	6.592	.0128	.0018
20°	8.00	5.824	.0129	.0015
25°	8.00	7.460	.0129	.0018

Figure 1.- Sketch of typical model.

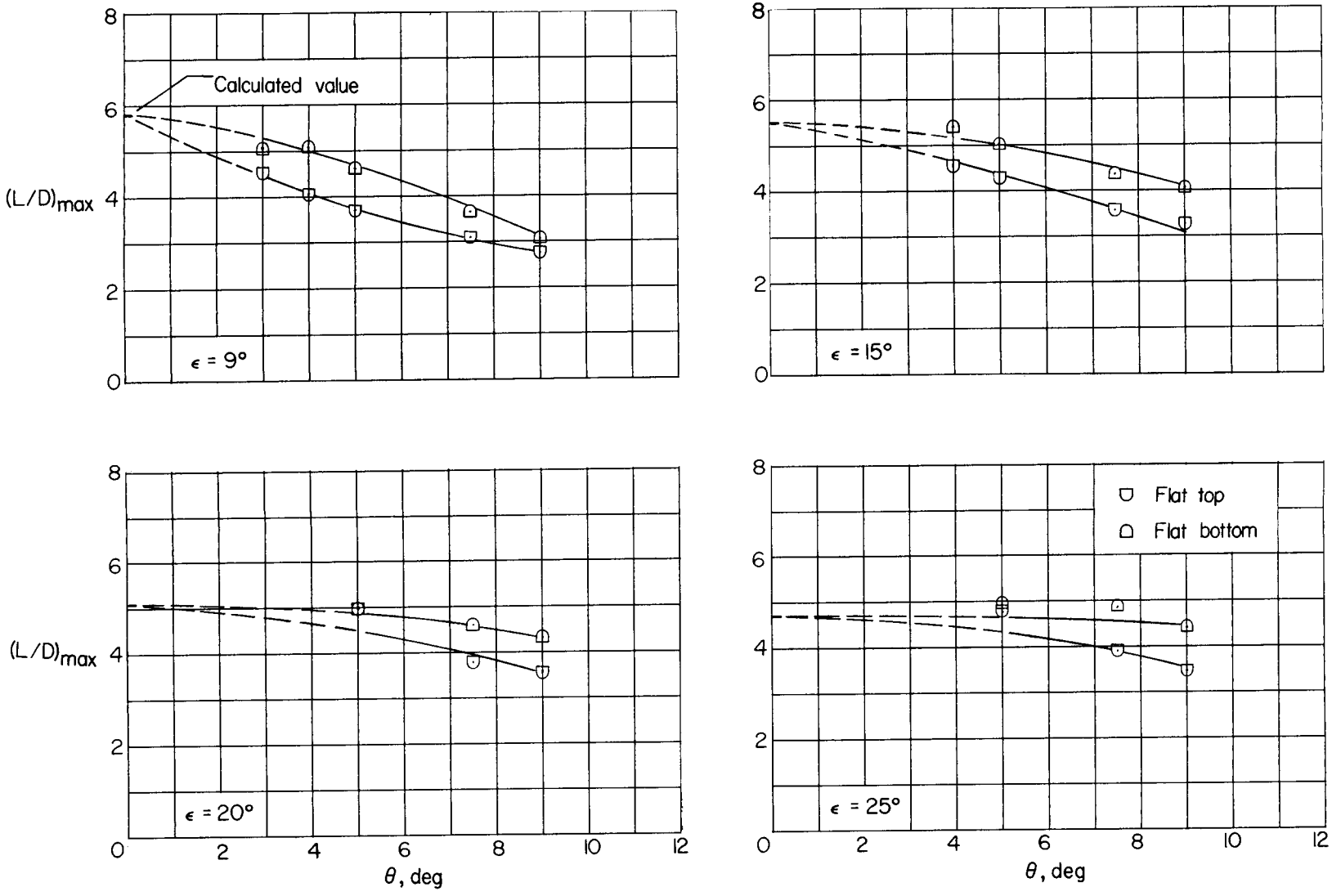

Figure 2.- Effect of half-cone angle on maximum lift-drag ratio. $R = 3.5 \times 10^6$.

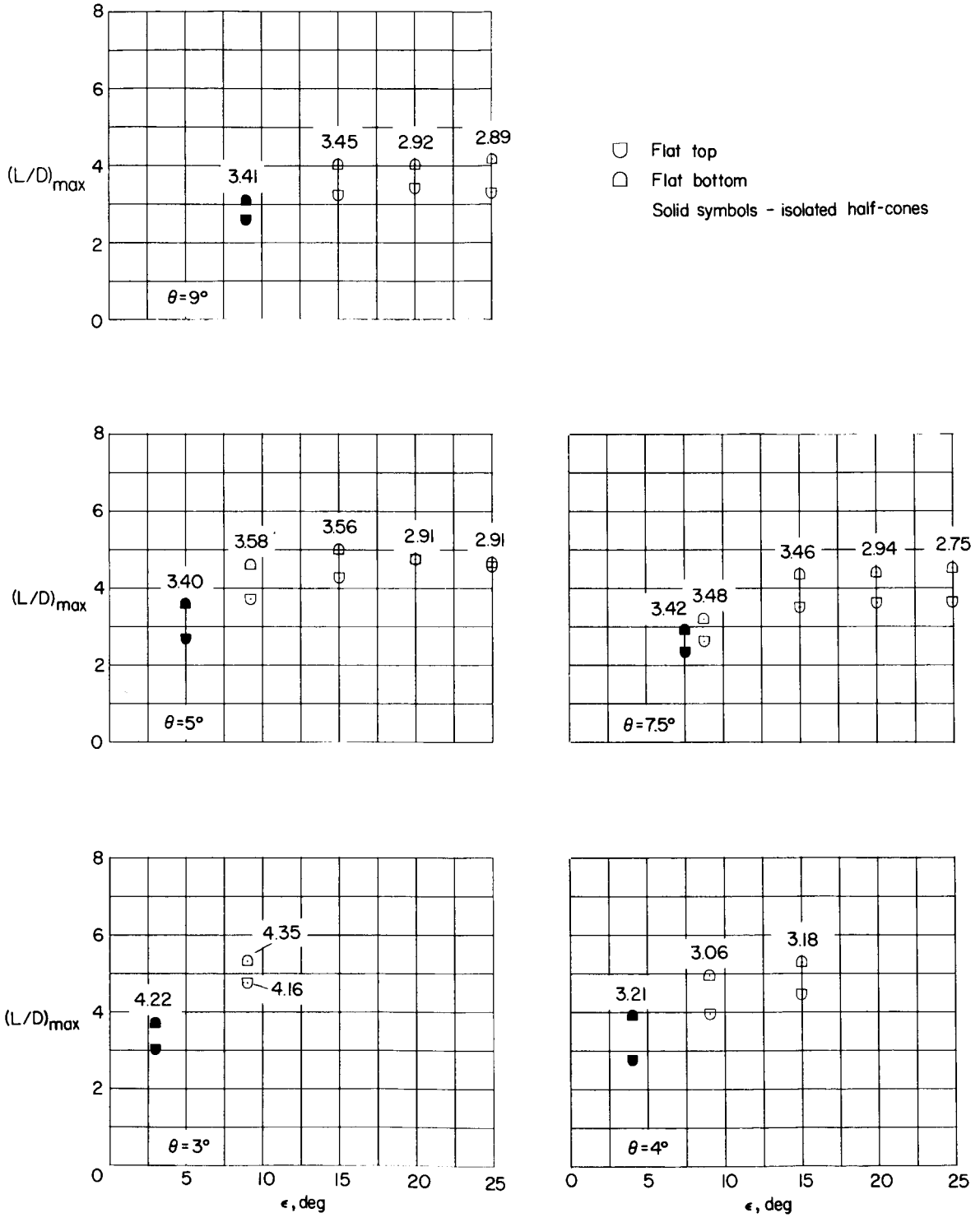

Figure 3.- Effect of wing semiapex angle on maximum lift-drag ratio. Figures adjacent to symbols represent test Reynolds number in millions.

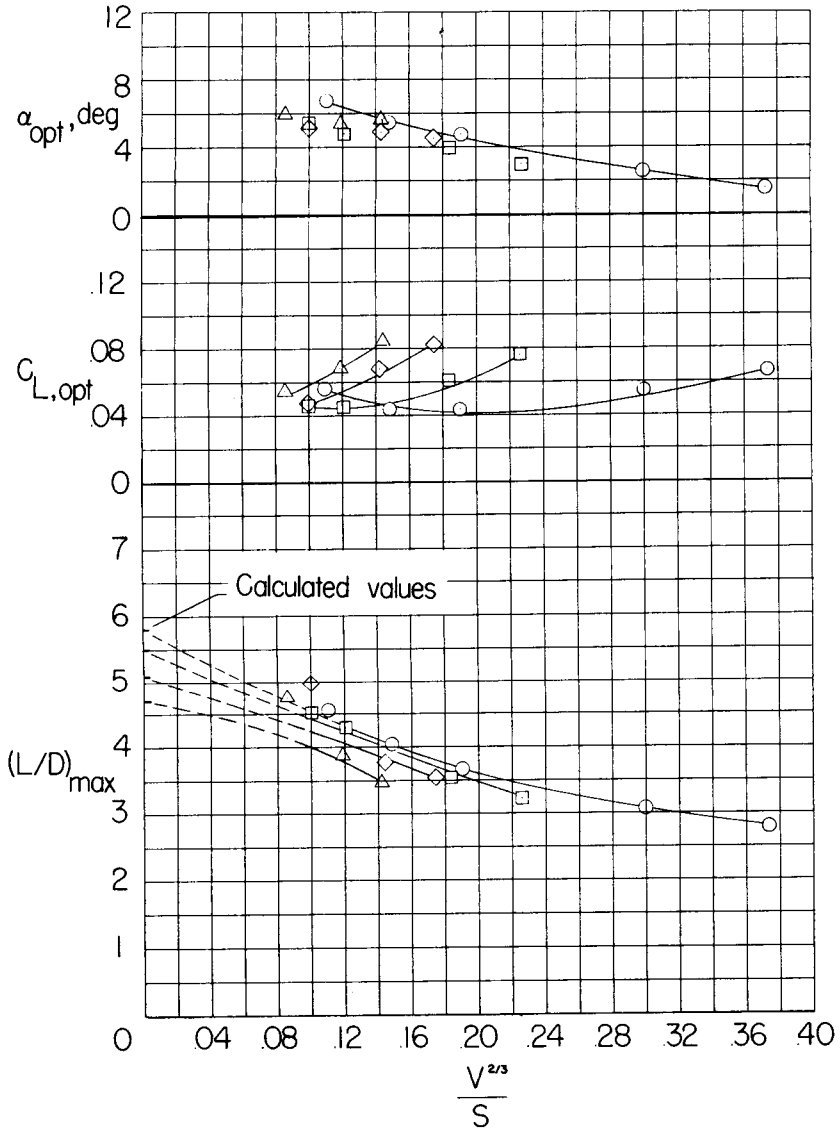

(a) Flat-top configuration.

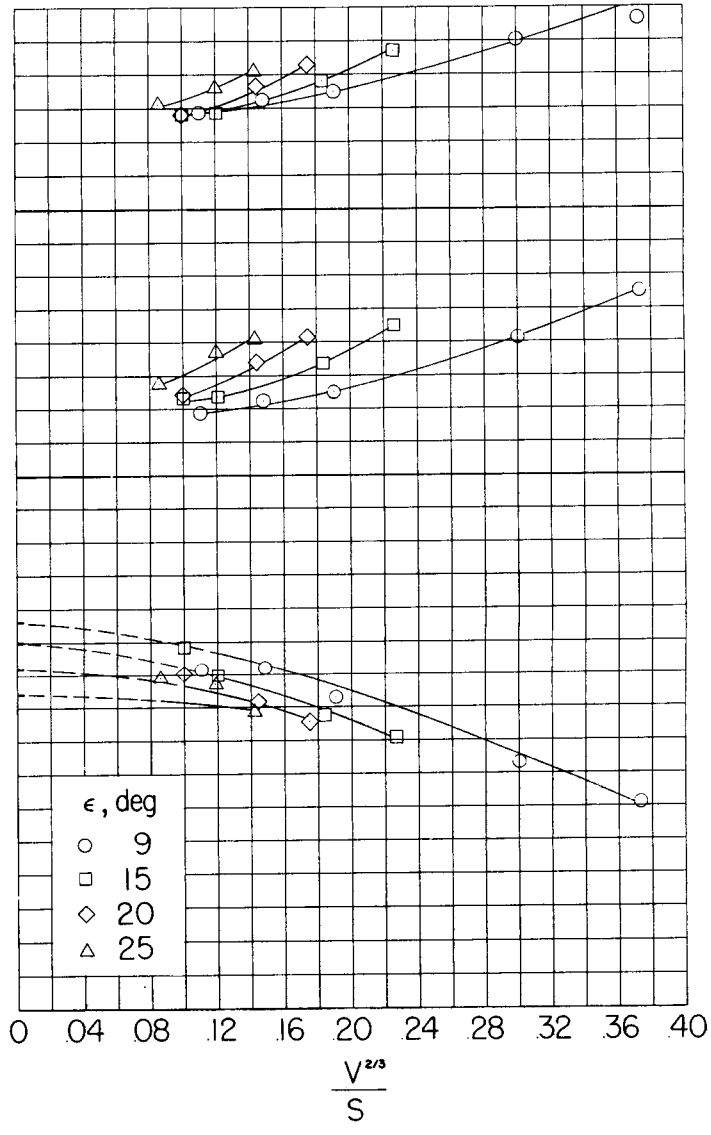

(b) Flat-bottom configuration.

Figure 4.- Performance of wing-body combinations as a function of volume coefficient. $R = 3.5 \times 10^6$.

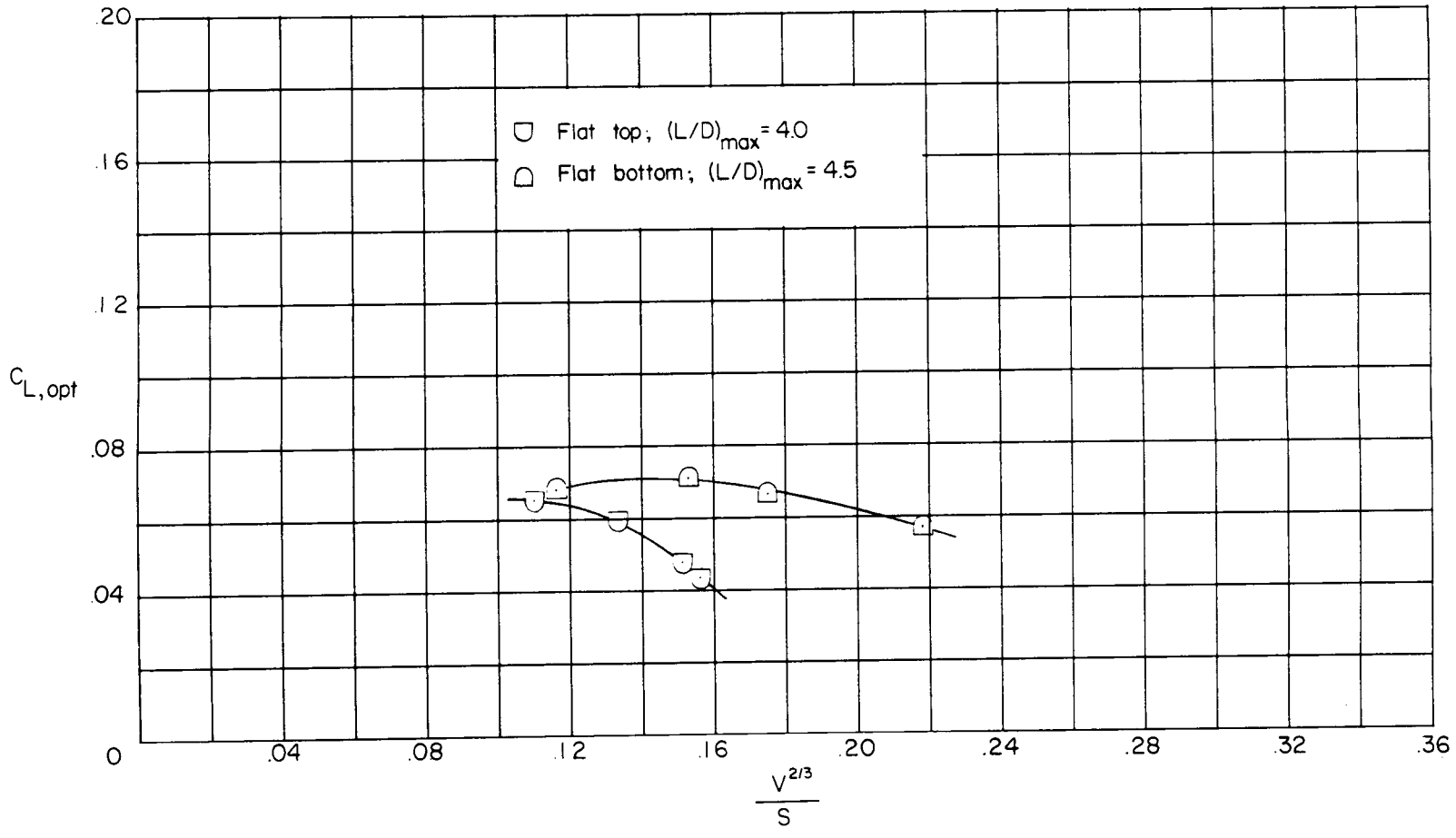

Figure 5.- Effect of volume coefficient on optimum lift coefficient for fixed lift-drag ratios.

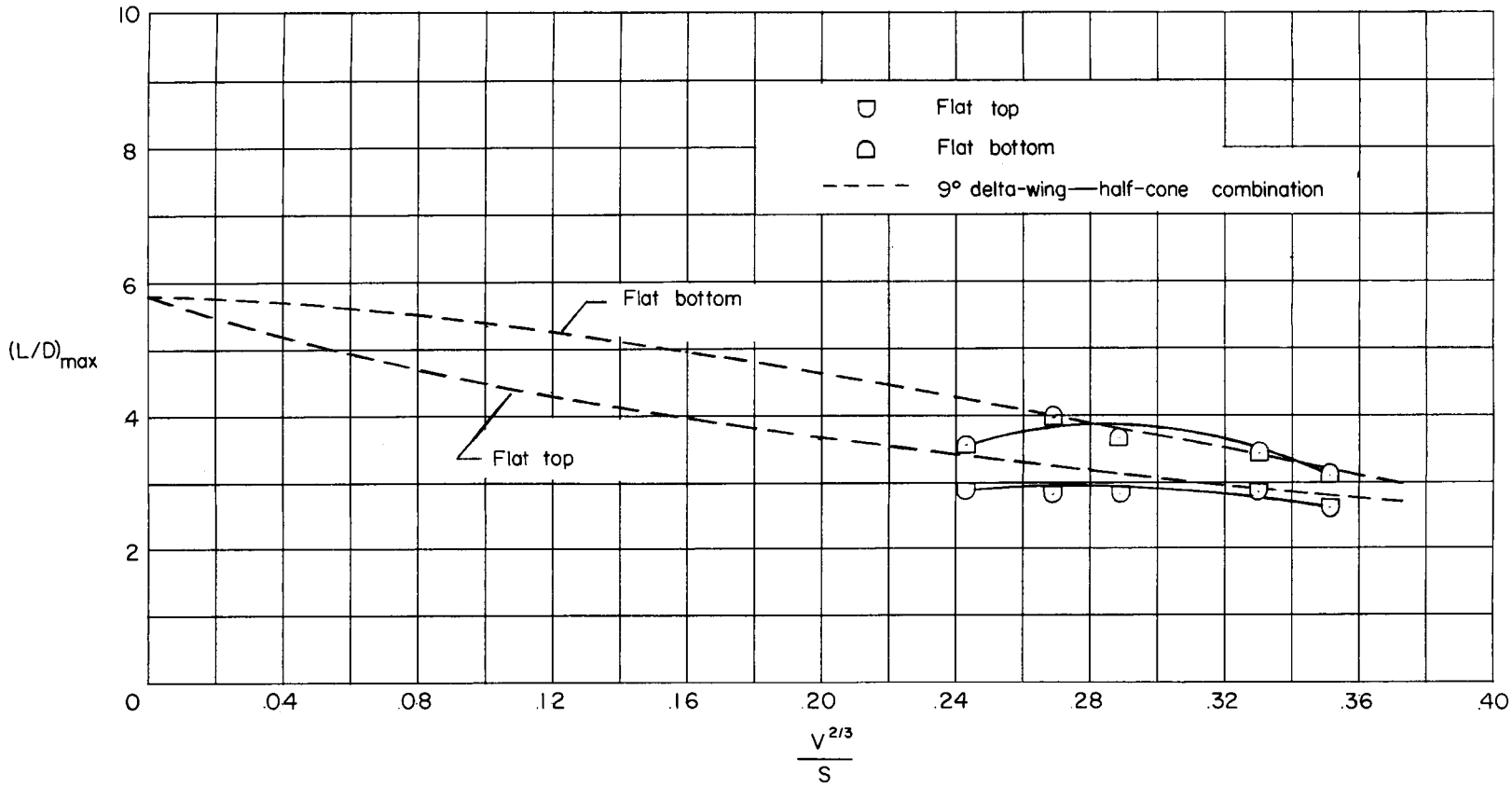

Figure 6.- Maximum lift-drag ratios of isolated half-cone bodies. M = 20; R = 3.5×10^6.

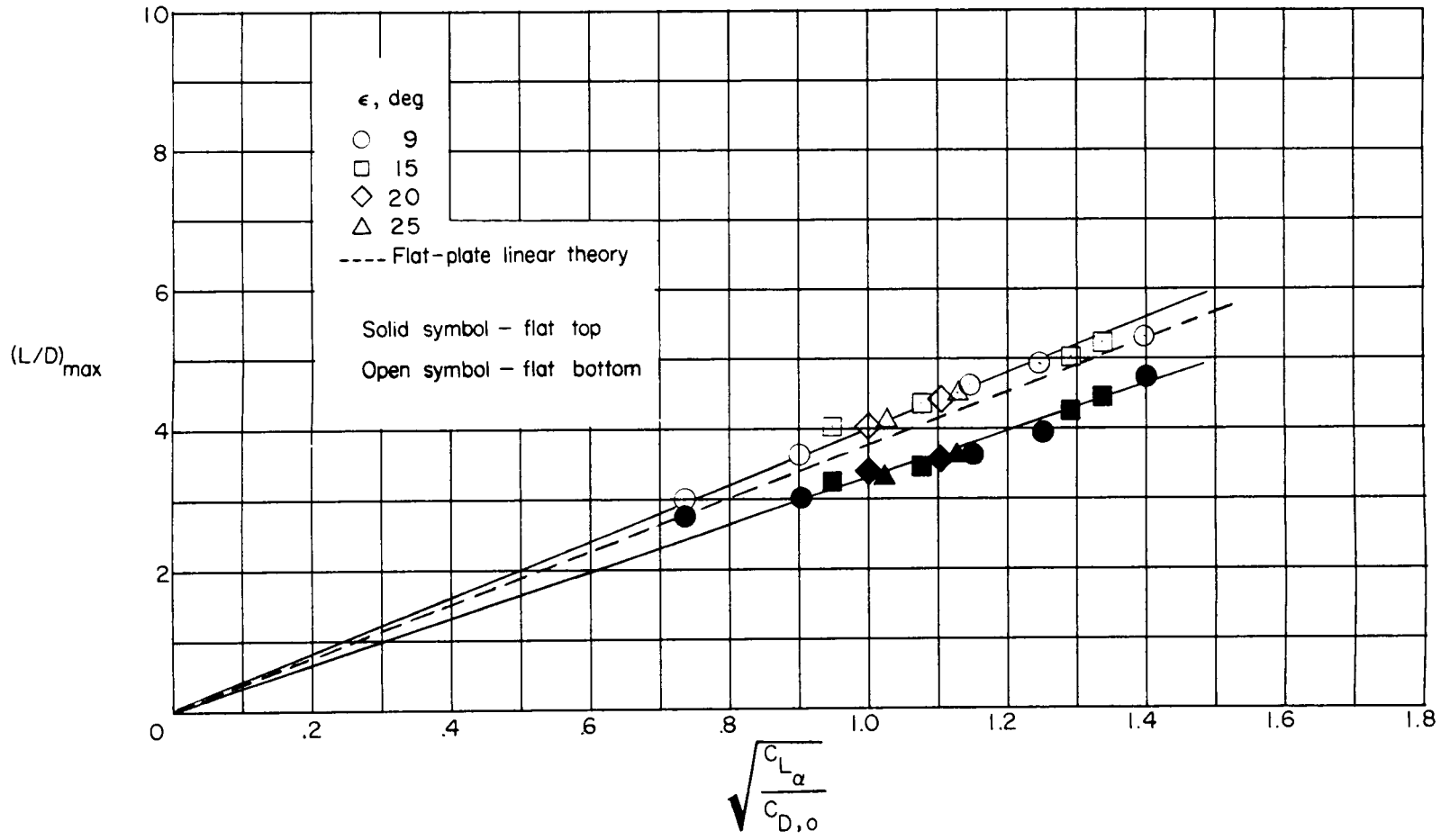

Figure 7.- Correlation of experimental maximum lift-drag ratios based on linear theory.

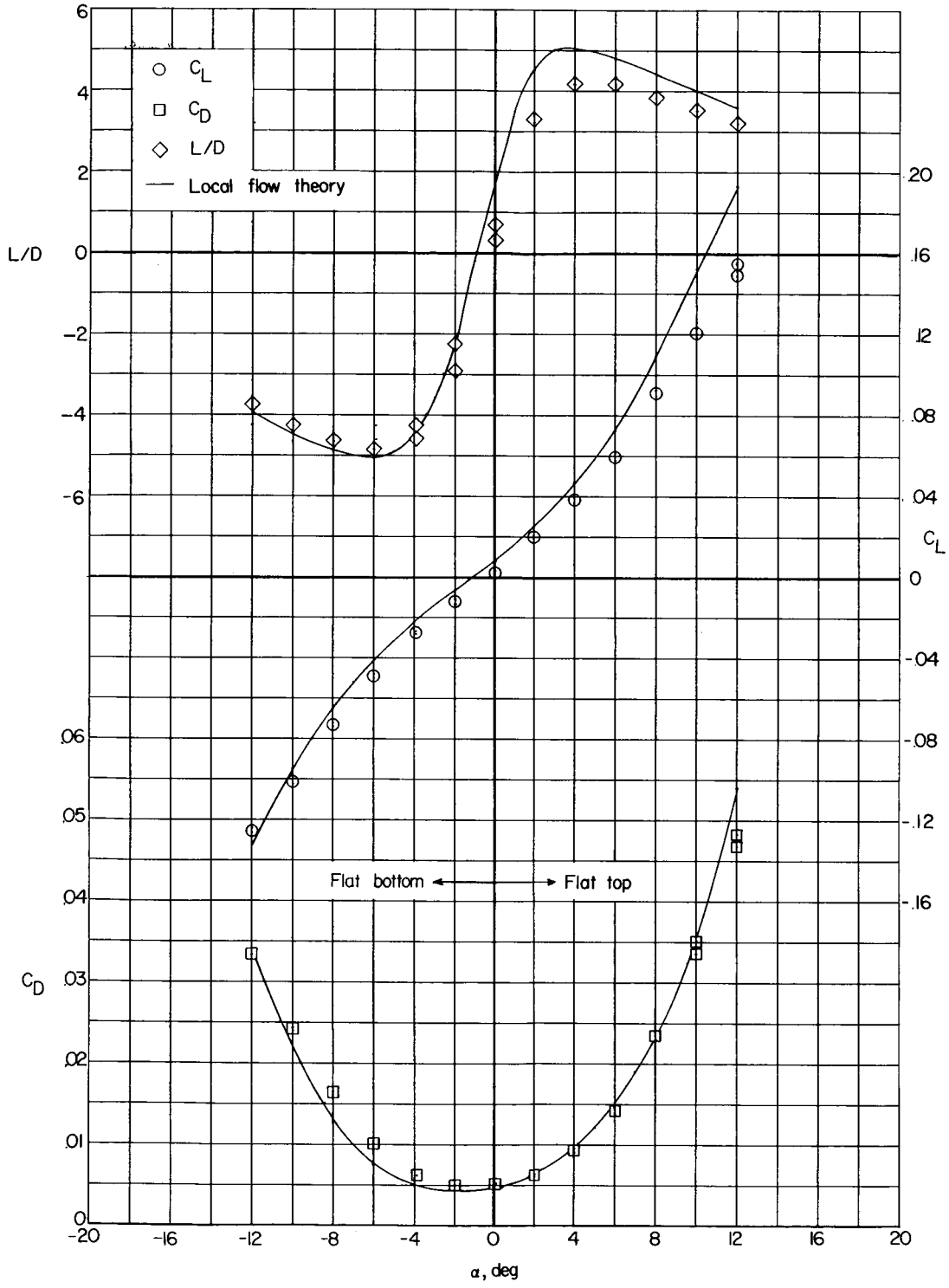

Figure 8.- Comparison of experimental results and local flow method of predicting performance. $\epsilon = 15^{\circ}$; $\theta = 5^{\circ}$.